

Electron Transport Properties and Device Applications of Nanocrystalline Silicon Quantum Dots

H. Mizuta^{1,6}, M. Khalafalla^{3,6}, Z. A.K. Durrani^{3,6}, S. Uno^{4,6}, N. Koshida^{5,6}, Y. Tsuchiya^{2,6} and S. Oda^{2,6}

¹Department of Physical Electronics, and ²Quantum Nanoelectronics Research Center, Tokyo Institute of Technology, Tokyo, Japan

³Microelectronics Research Centre, University of Cambridge, Cambridge, UK

⁴Hitachi Cambridge Laboratory, Cambridge, UK

⁵Faculty of Technology, Tokyo University of Agriculture and Technology, Tokyo, Japan

⁶CREST, JST (Japan Science and Technology)

This paper presents an overview on recent topical studies on electron transport properties and device applications of nanocrystalline silicon (nc-Si) quantum dots.

(1) Inter-dot coupling effects in nc-Si SETs

Electrostatic and coherent coupling effects between two adjacent nc-Si grains were studied by using point-contact single-electron transistors (PC-SETs: the inset to Fig.1). The PC-SETs with a very small channel with 30 nm × 30 nm × 40 nm in dimensions were formed on a 40 nm thick nc-Si film with lateral grain size of 20 – 25 nm. The electrostatic potential on the grains are controlled via the bias applied to two side gates. After patterning the PC-SETs, oxidation at 750°C for 60 minutes and annealing at 1000°C were applied, which convert the grain boundary (GB) into a solid tunnel barrier [1]. We observed the switching of the Coulomb oscillation current peaks at 4.2K [2], and the phenomenon was successfully reproduced using the Monte Carlo single-electron circuit simulation with a model of two parallel, capacitively-coupled Si dots.

Next we adopted oxidation at 750°C for 30 minutes without the following annealing in order for making the GB tunnel barrier more transparent so that the adjacent grains couple each other more tightly. The PC-SETs then exhibited delocalisation of the electron wavefunctions over the coupled grains. In the strong coupling region (a dotted circle in Fig.1), we observed that the characteristics are decomposed into four Lorentzian peaks – two main peaks with two small peaks. This is attributed to the tunnel coupling across two adjacent Si grains, resulting in bonding- and anti-bonding-like resonance peaks.

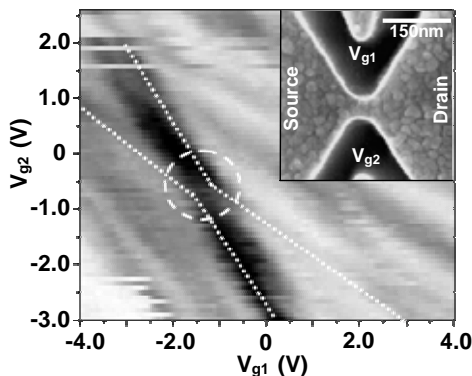


Fig. 1 SEM micrograph of a nano-Si point contact transistor (inset) and gray scale image of current as a function of two side gate bias voltages V_{g1} and V_{g2} .

(2) Phononic bandgap in a Si quantum dot linear array

Electron transport properties of the Si quantum dots interconnected with thin oxide layers have recently attracted growing attention due to the experimental observation of ballistic electron emission [3]. We investigated phononic states and electron-phonon

interactions theoretically for the 1D array of the Si quantum boxes of 4nm per side, interconnected with softer oxide layers of 1nm. The electron minibands were calculated using the Kronig-Penny potential, and the phonon normal modes were numerically calculated using the atomic linear chain model [4].

The calculation shows that the phonon dispersion curve has the energy gaps (phononic bandgaps) and the high-energy optical phonons are virtually dispersionless, which indicates the optical phonons are confined in the Si dots. Consequently, the electron-phonon interactions differ significantly from those for bulk Si: the acoustic phonon scattering potential is reduced and the inter-miniband scattering is prohibited as the electronic miniband gaps are larger than the maximum available phonon energy. These phenomena may lead to less electron energy dissipation in the system.

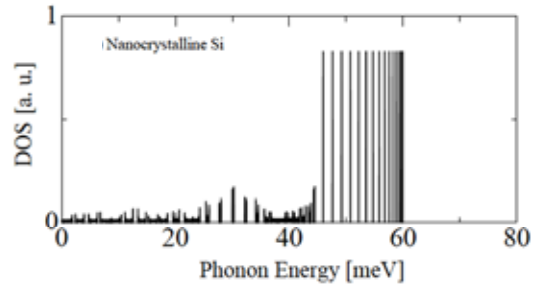


Fig. 2 Phonon density of states for the nc-Si dot array

(3) Nc-Si dot nonvolatile nanoelectromechanical memory

We recently proposed a new nonvolatile memory concept based on bistable operation of the NEMS structure combined with the nc-Si quantum dots (the inset to Fig.3). It features a suspended beam, which incorporates the nc-Si dots as single-electron storage. The beam may be moved via the gate electric field, and its positional displacement is sensed via a change in the drain current of the MOSFET underneath. The switching speed between two stable states was estimated to be ~ 0.5 ns for a SiO₂ beam with the dimension of 1.0 × 1.0 × 0.1 μm³, from a mechanical analysis assuming the maximum central displacement of 35 nm.

A free-standing SiO₂ beam was fabricated successfully using a Si undercut etching technique. Most fabricated samples showed upward-bent beams as a result of release of mechanical stress stored in SiO₂. The mechanical bistability of the beam was studied by using the nano-indenter type loading system. After the beam was loaded with the tip, we observed the beam was deformed to downward bent. These results indicate that a mechanically bistable SiO₂ beam can be formed by combining the conventional Si processes, and the bistable states can be switched by applying an external force.

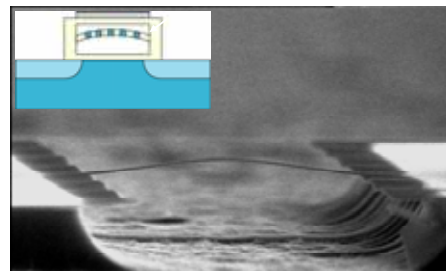


Fig. 3 An upward bent suspended SiO₂ beam and a schematic cross sectional view of the NEMS memory.

[1] Y. T. Tan *et al.*, J. Appl. Phys. 94, 633 (2003)
 [2] M. Khalafalla *et al.*, IEEE Nanotech. 2, 271 (2003).
 [3] N. Koshida *et al.*, Appl. Surf. Sci., 146, 371 (1999).
 [4] S. Uno *et al.*, IEEE Trans. Nanotechnol. 2, 301 (2003)